A Multiply Parasitic-Coupled, Three-Dimensional Antenna Array with Wide Elevation Angle for Seamless UAV Communications

Dong-Geun Seo and Wang-Sang Lee

Department of Electronic Engineering/Engineering Research Institute (ERI)
Gyeongsang National University (GNU), 501, Jinju-daero, Jinju, Gyeongnam, 52828, Republic of Korea
wsang@gnu.ac.kr

Abstract ─ A multiply parasitic-coupled, three-dimensional antenna array with wide elevation angle for seamless unmanned aerial vehicle (UAV) communications is proposed. The proposed array consists of an upper substrate with a two-element dipole array, multiple parasitic elements, two supports including a microstrip feeding, and a lower substrate with a feeding network and its ground plane as a metallic reflector for wide radiation pattern and reduced back radiation. The proposed array operates with a 18% impedance bandwidth ranging from 4.51 GHz to 5.43 GHz by covering an UAV communications frequency band. Measured peak gain, total efficiency, and half-power beamwidth (HPBW) of the proposed array are approximately 5.5 dBi, 95%, and 140°, respectively.

Index Terms ─ Antenna array, parasitic-coupled, three-dimensional antenna, UAV, wide elevation angle.

I. INTRODUCTION

Since unmanned aerial vehicles (UAVs) are able to remote control without people in aircraft, various applications using UAVs have been researched and expanded and have grown extensively over the years. In the military, UAVs utilize not only surveillance activities but also search-attack missions by focusing on the specific places or target objects. Furthermore, recent radio frequency identification (RFID) technology utilizes the UAVs for indoor or outdoor warehouse inventory management system in civilian industry. To realize these applications, the development of the customized antenna for reliable and stable UAV-based wireless communications is required. First of all, the UAV antenna requires a compact size such as lightweight and low-profile structure for stable long-time flight and communications. Secondly, it needs to have a symmetrical structure to balance the aircraft. Moreover, high gain and wide beam coverage are required to seamless UAV to UAV or UAV to infra communications. To satisfy these demands, previous researches have been studied in [1]–[7]. Crossed dipole loaded with magneto-electric dipole antenna is proposed in [1], [2]. The antenna with a metallic cavity has a wide axial-ratio (AR) beamwidth and a high front-to-back ratio [3]. In [4] and [5], the low-profile antenna with wide beamwidth is proposed utilizing the vertical currents. Using reconfigurable feeding network [6] and shorted vertical plates [7], the wide beams are generated. Although these antennas have achieved wide beamwidth and a low-profile structure, they have a low productivity and are not suitable for use in UAVs because their structures are complicated. In this paper, a lightweight, low-profile dipole antenna array with wide elevation angle using multiple parasitic elements is proposed for seamless UAV communications.

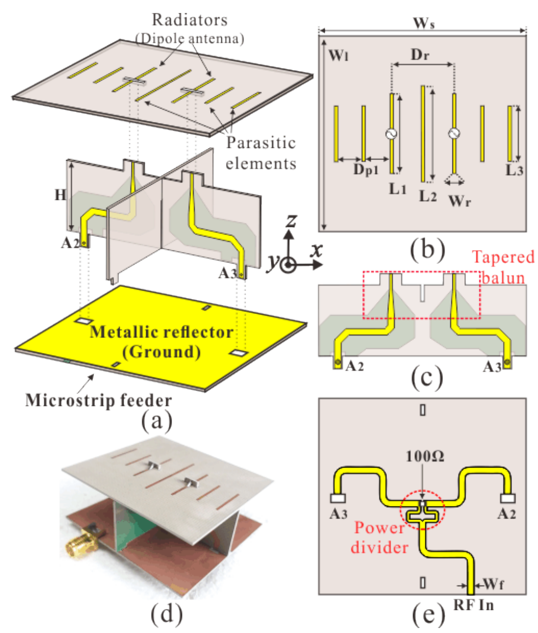

Fig. 1. Configuration of the proposed antenna array and its fabrication: (a) a perspective view of the proposed antenna array, (b) a top view of the upper substrate with dipole array and parasitic elements, (c) a top view of the antenna support with microstrip lines and a tapered balun, (d) the proposed array prototype, and (e) a bottom view of the lower substrate with a microstrip feeder.

Submitted On: December 26, 2019
Accepted On: April 12, 2020

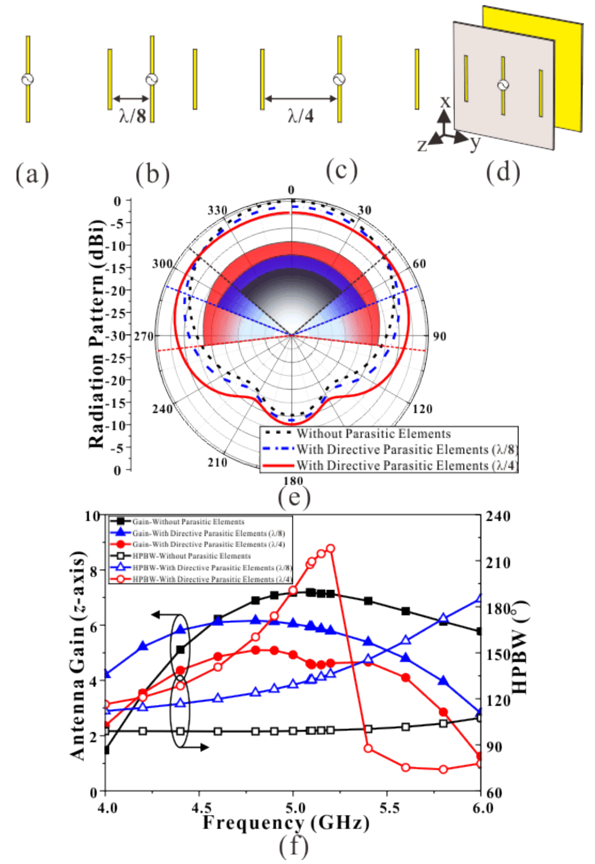

Fig. 2. Performance analysis of the antenna with or without parasitic elements: (a) a dipole antenna without parasitic element, (b) a dipole antenna with two parasitic elements of $\lambda_0/8$, (c) a dipole antenna with two parasitic elements of $\lambda_0/4$, (d) a simulation model for the proposed antenna, (e) radiation patterns and HPBWs with regard to the antenna structure, and (f) antenna gain at the main-beam direction and HPBW with regard to frequency variations.

II. PROPOSED ANTENNA ARRAY WITH A FEEDING CIRCUIT

Based on the linear array antenna theory, the proposed antenna array is based on a two-element dipole antenna array which has broadside beam [8]. Each unit cell antenna operates with the same power and a zero-phase difference. Figure 1 indicates the proposed antenna configuration and its fabricated array prototype. The proposed array consists of an upper substrate, a lower substrate, and two supports in Fig. 1 (a). The upper substrate includes a two-element dipole antenna array and five-parasitic elements with directive and reflective parasitic elements. Parasitic elements are added to widen an elevation beamwidth. To increase the directivity, a ground plane at the top layer on the lower substrate operates as a metallic reflector, and the bottom layer has a feeding network. It consists of a power divider and microstrip lines for feeding the two-element dipole array. To obtain the maximum antenna performance, the separated distance between upper and lower substrates is the height of the supports, and printed microstrip lines and tapered baluns are connected to the radiators. Figures 1 (b) and 1 (c) depict the top view of the upper substrate and antenna supports with a microstrip feeding, respectively. Figures 1 (d) and 1 (e) show the fabricated antenna prototype and the bottom view of the lower substrate, respectively. Table 1 describes the design parameters of the proposed array.

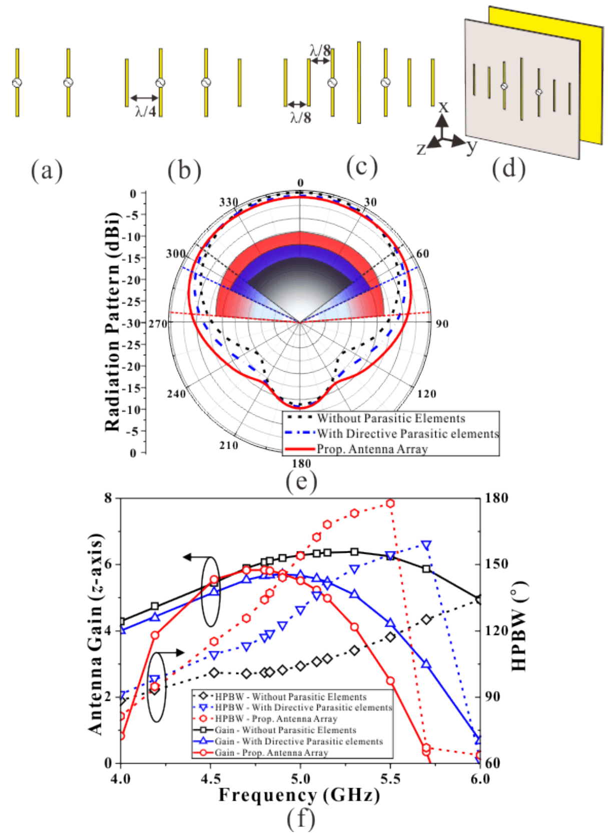

Fig. 3. Comparison between the dipole array with and without parasitic elements: (a) a two-element dipole array without parasitic elements, (b) a two-element dipole array with two parasitic elements, (c) a two-element dipole array with five parasitic elements, (d) a simulation model for the proposed antenna, (e) simulated radiation patterns with regard to the parasitic elements, and (f) simulated antenna gain and HPBW at *z*-axis with regard to the parasitic elements.

Table 1: Design parameters of the proposed array (unit: *mm*)

W_s	W_l	H	D_{p1}	D_r
56	53	20	7.5	17
L_1	L_2	L_3	W_r	W_f
21.4	28	14	0.7	1.78

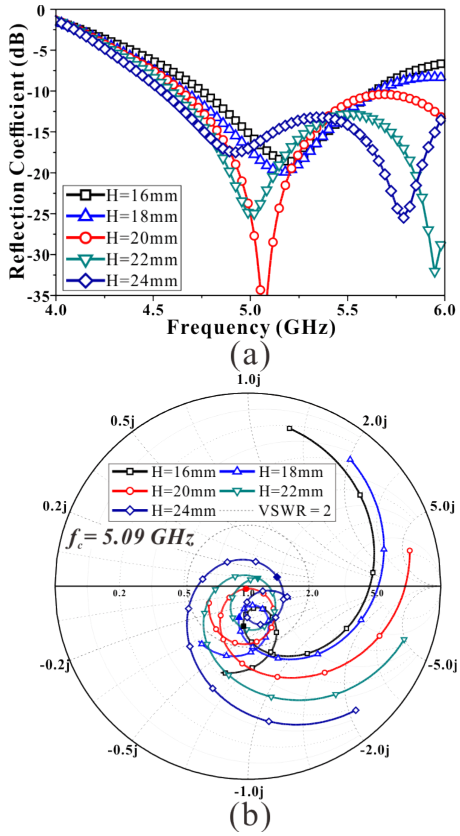

Fig. 4. Simulated impedance variation at operating frequency with regard to H: (a) reflection coefficient variation and (b) impedance variation on Smith chart.

Figure 2 depicts the performance analysis of the different antenna structures with regard to the separated distance between radiators and parasitic elements. Figurees 2 (a)-(c) indicate a dipole antenna, dipole antenna with directive parasitic elements at intervals of λ_0 /8, and a dipole antenna with directive parasitic elements at intervals of λ_0/4, respectively. The simulation has been conducted using an antenna deployment in Fig. 2 (d). It consists of the radiating substrate and a metallic reflector. The simulated radiation patterns and half-power beamwidth (HPBW) at 5.09 GHz are in Fig. 2 (e). As the parasitic elements are far from the dipole antenna, HPBW is increased but the gain is reduced at 0° due to the trade-off between the gain and beamwidth. Similarly, Fig. 2 (f) shows the gain and HPBW with regard to the operating frequency. The antenna gain is decreased and HPBW is increased when the operating frequency increases and the parasitic elements are separated. In particular, the radiated beams are splitted at 5.03 GHz of λ_0/4 deployment.

On the other hand, in order to compare HPBW at the elevation plane with regard to multiple parasitic elements, Figs. 3 (a)–(c) describe the different antenna array deployments with or without multiple parasitic elements. Figure 3 (d) indicates the simulation model for the proposed antenna. Figure 3 (e) shows the simulated radiation patterns of the dipole array with or without two parasitic elements and the proposed antenna array, respectively. The multiply parasitic elements increase the HPBW at elevation plane. The proposed antenna array in Fig. 3 (c) has a wide beamwidth of approximately 162° rather than 106° and 136° at 5.09 GHz in Figs. 3 (a) and 3 (b), respectively. Other comparisons are conducted to compare the antenna gain and HPBW at *z*-axis with regard to the parasitic elements in Fig. 3 (f). As frequency increases, the HPBW also increases. However, the gain is rather reduced at higher than 5.7 GHz due to the beam splitting. Therefore, the proposed antenna array has been optimized for wide elevation angle and the antenna gain at UAV frequency band.

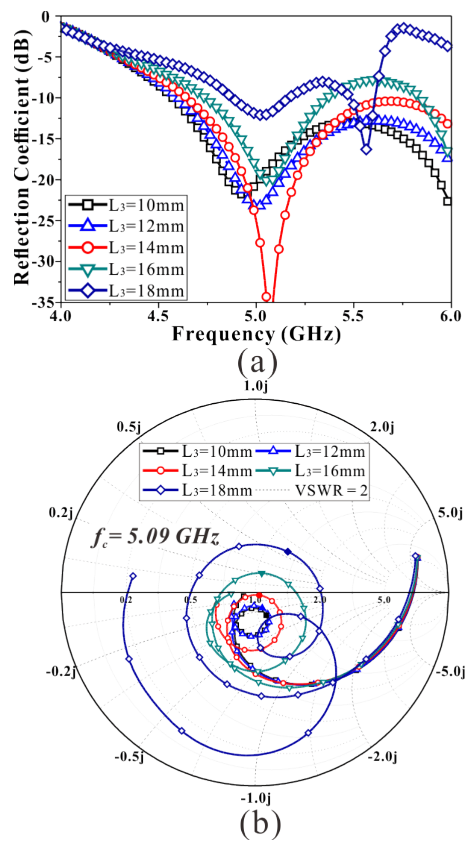

Fig. 5. Simulated impedance variation with regard to L_3: (a) reflection coefficient variation with regard to frequency, and (b) impedance variation on Smith chart.

III. RESULTS AND DISCUSSIONS

The proposed antenna array operates in the UAV communication frequency band from 5.03 GHz to 5.15 GHz, which is assigned to the World Radio communication Conference-12 (WRC) of International Telecommunication Union (ITU). It is simulated and optimized using a commercial full-wave electromagnetic simulation tool (Microwave Studio 2019 by CST), and designed and fabricated on an RF-35 substrate (ε_r = 3.5, δ = 0.0018) for experimental verifications. To obtain the mutual effect between the upper and lower substrates, the simulated results with regard to the antenna height (H) variations is shown in Fig. 4. The reflection coefficient with regard to the operating frequency is described in Fig. 4 (a). The resonant frequency is increased by reducing *H*. Figure 4 (b) shows the variation of reflection coefficients on Smith chart, and it describes the impedance increases when *H* increases. Similarly, the proposed array is affected by the director length (L_3) in Fig. 5. As the L_3 increases, its resonant frequency and impedance on Smith chart are increased. By considering the antenna gain, radiation patterns with wide beamwidth, and the reflection coefficients, the geometry of the proposed array with multiple parasitic elements is determined on Table 1.

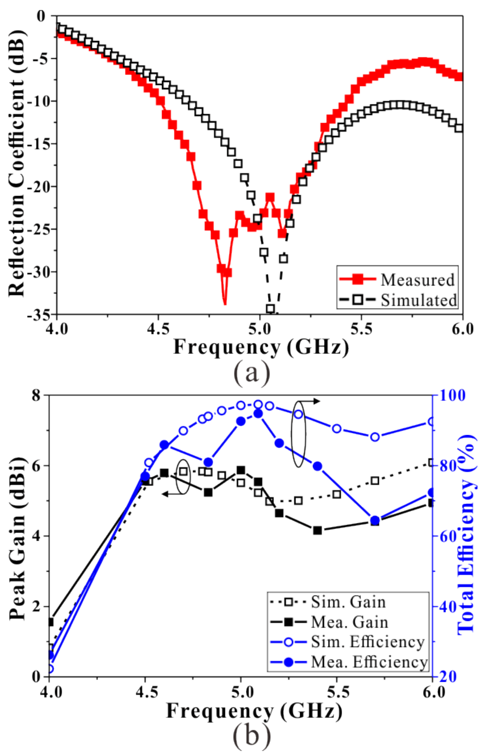

Fig. 6. Simulated and measured antenna performances: (a) reflection coefficient with regard to operating frequency and (b) peak gain and total efficiency with regard to operating frequency.

Figure 6 shows simulated and measured results of reflection coefficient, peak gain, and total efficiency. The measured 10-dB bandwidth is approximately 18% from 4.51 GHz to 5.43 GHz. The difference between simulated and measured results is caused by the implementation error of three-dimensional antenna. The measured peak gain and total efficiencies in Fig. 6 (b) are approximately 5.54 dBi and 95% at 5.09 GHz, respectively. Figure 7 indicates the simulated and measured radiation patterns, which are a good agreement between the simulated and measured results. The HPBW and cross-polarization level of the proposed array are approximately 140° and -23 dB, respectively. Table 2 describe the performance comparison between the previous works and the proposed array. The proposed antenna has relatively wide beam coverage and a high gain.

Table 2: Performance comparison between the previous works and the proposed array

Ref.	f_c (GHz)	Imp. BW (MHz)	Peak Gain (dBi(c))	HPBW (°)	Elect. Size (λ^3)
[1]	1.8	970	8.3	70	0.64×0.64×0.16
[2]	4	600	3.5	221	0.43×0.43×0.24
[3]	1.6	1160	3.4	116	0.35×0.35×0.06
[5]	1.5	1170	4.5	110	0.46×0.46×0.1
[6]	2.55	600	7	120	1.45×1.45×0.12
[13]	2	500	5.5	136	1.58×1.14×0.25
Prop.	**5.09**	**920**	**5.5**	**140**	**0.95×0.9×0.34**

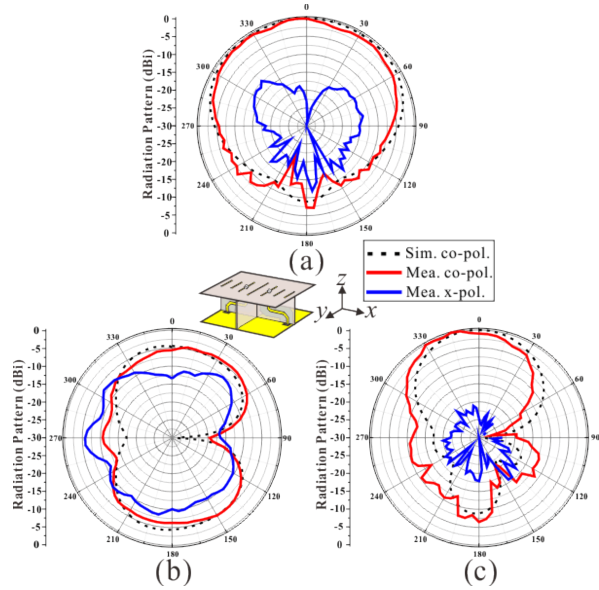

Fig. 7. Simulated and measured radiation patterns with co-polarization and cross-polarization: (a) *zx*-plane, (b) *xy*-plane, and (c) *zy*-plane.

IV. CONCLUSION

A multiply parasitic-coupled, three-dimensional antenna array with wide elevation angle for seamless UAV communication is presented in this paper. Based on the linear array antenna theory, a wide beam-coverage at elevation plane is obtained using a two-element dipole array and parasitic elements. Measured peak gain and

HPBW of the proposed array are approximately 5.5 dBi and 140°, respectively Due to a symmetrical structure, a low-profile configuration, and a wide elevation angle, the proposed antenna array is attractive to various wireless communications systems as well as UAV communications.

ACKNOWLEDGMENT

This work was supported in part by Institute for Information & communications Technology Promotion (IITP) grant funded by the Korea government (MSIT) (No. 2017-0-00795, A study on a small antenna system for vehicle supporting wide elevation angle), in part by the National Research Foundation of Korea (NRF) Grant funded by the Korea government (MSIT) (No. 2019R1C1C1008102).

REFERENCES

[1] S. X. Ta and I. Park, “Crossed dipole loaded with magneto-electric dipole for wideband and wide-beam circularly polarized radiation,” *IEEE Antennas Wireless Propag. Lett.*, vol. 14, pp. 358-361, 2015.

[2] G. Yang, J. Li, S. G. Zhou, and Y. Qi, “A wide-angle E-plane scanning linear array antenna with wide beam elements,” *IEEE Antennas Wireless Propag. Lett.*, vol. 16, pp. 2923-2926, 2017.

[3] L. Wang, Z. Weng, Y. Jiao, W. Zhang, and C. Zhang, “A low-profile broadband circularly polarized microstrip antenna with wide beamwidth,” *IEEE Antennas Wireless Propag. Lett.*, vol. 17, no. 7, pp. 1213-1217, July 2018.

[4] X. Chen, L. Yang, J. Zhao, and G. Fu, “High-efficiency compact circularly polarized microstrip antenna with wide beamwidth for airborne communication,” *IEEE Antennas Wireless Propag. Lett.*, vol. 15, pp. 1518-1521, 2016.

[5] W. J. Yang, Y. M. Pan, and S. Y. Zheng, “A low-profile wideband circularly polarized crossed-dipole antenna with wide axial-ratio and gain beamwidths,” *IEEE Trans. Antennas Propag*., vol. 66, no. 7, pp. 3346-3353, July 2018.

[6] W. Lin, H. Wong, and R. W. Ziolkowski, “Wideband pattern-reconfigurable antenna with switchable broadside and conical beams,” *IEEE Antennas Wireless Propag. Lett*., vol. 16, pp. 2638-2641, 2017.

[7] G. Li and F. Zhang, “A compact broadband and wide beam circularly polarized antenna with shorted vertical plates,” *IEEE Access*, vol. 7, pp. 90916-90921, 2019.

[8] C. A. Balanis, *Antenna Theory, Analysis and Design*. New York, Wiley, 1997.

Dong-Geun Seo received the B.S. degree in Electronic Engineering from Gyeongsang National University (GNU), Jinju, South Korea, in 2016, where he is currently pursuing the M.S. degree. His current research interests include near-field wireless power transfer and communication systems, beamforming antenna array and its feeding network for UAV communications, and RFID/IoT sensors.

Wang-Sang Lee received the B.S. degree from Soongsil University, Seoul, South Korea, in 2004, and the M.S. and Ph.D. degrees in Electrical Engineering from the Korea Advanced Institute of Science and Technology (KAIST), Daejeon, South Korea, in 2006 and 2013, respectively.

From 2006 to 2010, he was with the Electromagnetic Compatibility Technology Center, Digital Industry Division, Korea Testing Laboratory (KTL), Ansan-si, South Korea, where he was involved in the international standardization for radio frequency identification (RFID) and photovoltaic systems as well as electromagnetic interference (EMI)/EMC analysis, modeling, and measurements for information technology devices. In 2013, he joined the Korea Railroad Research Institute (KRRI), Uiwang-si, South Korea, as a Senior Researcher, where he was involved in the position detection for high-speed railroad systems and microwave heating for low-vibration rapid tunnel excavation system. Since 2014, he has been an Associate Professor with the Department of Electronic Engineering, Gyeongsang National University (GNU), Jinju, South Korea. From 2018 to 2019, he was a Visiting Scholar with the ATHENA Group, Georgia Institute of Technology, Atlanta, GA, USA. His current research interests include near- and far-field wireless power and data communications systems, RF/microwave antenna, circuit, and system design, RFID/Internet-of-Things (IoT) sensors, and EMI/EMC.

Lee is a member of IEC/ISO JTC1/SC31, KIEES, IEIE, and KSR. He was a recipient of the Best Paper Award at IEEE RFID in 2013, the Kim Choong-Ki Award: EE Top Research Achievement Award by the Department of Electrical Engineering, KAIST, in 2013, the Best Ph.D. Dissertation Award: the Department of Electrical Engineering, KAIST, in 2014, the Young Researcher Award by KIEES in 2017.